

Interplay of Structure and Reactivity in a Most Unusual Furan Diels-Alder Reaction

Gerry A. Griffith,[†] Ian H. Hillier,^{*‡} Andrew C. Moralee,[†] Jonathan M. Percy,^{*†,§}
Ricard Roig,[†] and Mark A. Vincent[‡]

Contribution from the Department of Chemistry, University of Leicester, University Road,
Leicester LE1 7RH, UK, and School of Chemistry, University of Manchester,
Oxford Road, Manchester M13 9PL, UK

Received March 2, 2006; E-mail: jonathan.percy@strath.ac.uk

Abstract: Difluorinated alkenoate ethyl 3,3-difluoro-2-(*N,N*-diethylcarbamoyloxy)-2-propenoate reacts rapidly and in high yield with furan and a range of substituted furans in the presence of a tin(IV) catalyst. Non-fluorinated congener 2-(*N,N*-diethylcarbamoyloxy)-2-propenoate fails to react at all under the same conditions. These reactions have been explored using density functional theory (DFT) calculations. They reveal a highly polar transition state, which is stabilized by the Lewis acid catalyst SnCl₄ and by polar solvents. In the presence of both catalyst and solvent, a two-step reaction is predicted, corresponding to the stepwise formation of the two new carbon–carbon bonds *via* transition states which have similar energies in all cases. Our experimental observations of the lack of reaction of the non-fluorinated dienophile, the stereochemical outcomes, and the rate acceleration accompanying furan methylation are all well predicted by our calculations. The calculated free energy barriers generally correlate well with measured reaction rates, supporting a reaction mechanism in which zwitterionic character is developed strongly. An *in situ* ring opening reaction of *exo*-cycloadduct ethyl *exo*-2-(*N,N*-diethylcarbamoyloxy)-3,3-difluoro-7-oxabicyclo[2.2.1]hept-5-enyl-2-*endo*-carboxylate, which results in the formation of cyclic carbonate ethyl 4,4-difluoro-5-hydroxy-2-oxo-5,7a-dihydro-4*H*-benzo[1,3]dioxole-3a-carboxylate by a Curtin–Hammett mechanism, has also been examined. Substantial steric opposition to Lewis acid binding prevents carbonate formation from 2-substituted furans.

1. Introduction

Diels–Alder reactions of propenoic (acrylic) acid derivatives with furan are well-known and extremely useful¹ though sometimes slow and low-yielding; the oxanorbornenes that they form are versatile templates from which a wide range of natural products can be constructed. Lewis acids² or high-pressure conditions³ can be used to improve reaction rates and yields significantly. Recently, Houk has studied the effect of the incorporation of halogen atoms into furans on their Diels–Alder reactions. This simple structural modification exerts a profound effect, converting a number of reactions which fail in the absence

of the halogen atom into successes.⁴ Strong continued interest in the synthesis and properties of selectively fluorinated molecules at the interface of chemistry and biomolecular science⁵ makes our attempts to adapt the strategically important and powerful reactions of modern synthetic organic chemistry⁶ to the presence of fluorinated substrates, and to understand the interplay of structure and reactivity, a worthwhile goal. The system studied in this manuscript is an extremely unusual one. At the start of our synthetic campaign, we found a solitary paper

[†] University of Leicester.

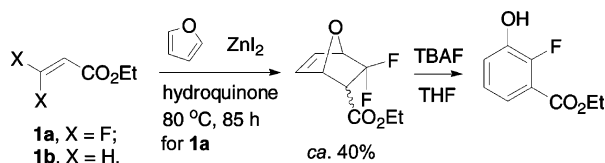
[‡] University of Manchester.

[§] Current address: Department of Pure and Applied Chemistry, WestCHEM, University of Strathclyde, Thomas Graham Building, 295 Cathedral Street, Glasgow G1 1XL, UK.

- (1) For reviews, see: (a) Woo, S.; Keay, B. A. *Synthesis* **1996**, 669. (b) Vogel, P.; Cossy, J.; Plumet, J.; Arjona, O. *Tetrahedron* **1999**, 55, 13521. (c) Vogel, P. *Curr. Org. Chem.* **2000**, 4, 455. (d) Arjona, O.; Plumet, J. *Curr. Org. Chem.* **2002**, 6, 571. (e) Lautens, M.; Fagnou, K.; Hiebert, S. *Acc. Chem. Res.* **2003**, 36, 48.
- (2) (a) The first effective Lewis acid for this reaction was ZnI₂; Brion, F. *Tetrahedron Lett.* **1982**, 23, 5299. (b) For more recent uses of a hafnium Lewis acid, see: Hayashi, Y.; Nakamura, M.; Nakao, S.; Inoue, T.; Shoji, M. *Angew. Chem., Int. Ed.* **2002**, 41, 4079.
- (3) (a) Kotsuki, H.; Nishizawa, H.; Ochi, M.; Matsuoka, K. *Bull. Chem. Soc. Jpn* **1982**, 55, 496. (b) For a compendium of reactions carried out under high pressure, see: Matsumoto, K.; Hamana, H.; Iida, H. *Helv. Chim. Acta* **2005**, 88, 2033.

- (4) Pieniazek, S. N.; Houk, K. N. *Angew. Chem., Int. Ed.* **2006**, 45, 1442.
- (5) For recent reviews of fluorinated molecules at the interface between chemistry and biomolecular science, see: (a) De Souza, M. V. N. *Mini-Rev. Med. Chem.* **2005**, 5, 1009. (b) Jackel, C.; Koksich, B. *Eur. J. Org. Chem.* **2005**, 4483. (c) Natarajan, R.; Azerad, R.; Badet, B.; Copin, E. *J. Fluorine Chem.* **2005**, 126, 425. (d) Deng, H.; O'Hagan, D.; Schaffrath, C. *Nat. Prod. Rep.* **2004**, 21, 773. (e) Qiu, X. L.; Meng, W. D.; Qing, F. L. *Tetrahedron* **2004**, 60, 6711. (f) Pongdee, R.; Liu, H. W. *Bioorg. Chem.* **2004**, 32, 393. (g) Yu, J. X.; Kodibagkar, V. D.; Cui, W. N.; Mason, R. P. *Curr. Med. Chem.* **2005**, 12, 819.
- (6) (a) Griffith, G. A.; Percy, J. M.; Pintat, S.; Smith, C. A.; Spencer, N.; Uneyama, E. *Org. Biomol. Chem.* **2005**, 3, 2701. (b) Cox, L. R.; DeBoos, G. A.; Fullbrook, J. J.; Percy, J. M.; Spencer, N. *Tetrahedron-Asymmetry* **2005**, 16, 347. (c) Audouard, C.; Fawcett, J.; Griffith, G. A.; Kerouredan, E.; Miah, A.; Percy, J. M.; Yang, H. L. *Org. Lett.* **2004**, 6, 4269. (d) Audouard, C.; Barsukov, I.; Fawcett, J.; Griffith, G. A.; Percy, J. M.; Pintat, S.; Smith, C. A. *Chem. Commun.* **2004**, 1526. (e) DiMartino, G.; Hursthouse, M. B.; Light, M. E.; Percy, J. M.; Spencer, N. S.; Tolley, M. *Org. Biomol. Chem.* **2003**, 1, 4423. For reviews describing other important synthetic strategies, see: (f) Rozen, S. *Eur. J. Org. Chem.* **2005**, 2433. (g) Rozen, S. *Acc. Chem. Res.* **2005**, 38, 803. (h) Shimizu, M.; Hiyama, T. *Angew. Chem., Int. Ed.* **2005**, 44, 214. (i) Ma, J. A.; Cahard, D. *Chem. Rev.* **2004**, 104, 6119. (j) Nyffeler, P. T.; Duron, S. G.; Burkart, M. D.; Vincent, S. P.; Wong, C. H. *Angew. Chem., Int. Ed.* **2005**, 44, 192.

Scheme 1



describing the synthesis of a difluorinated propenoate (acrylate) ester and its furan Diels–Alder reaction, in sharp contrast to the ubiquity of the reaction with non-fluorinated dienophiles. Wakselman and co-workers synthesized **1a** from dibromodifluoromethane and carried out both uncatalyzed and zinc-iodide-catalyzed cycloadditions with a moderate excess of furan (Scheme 1).⁷

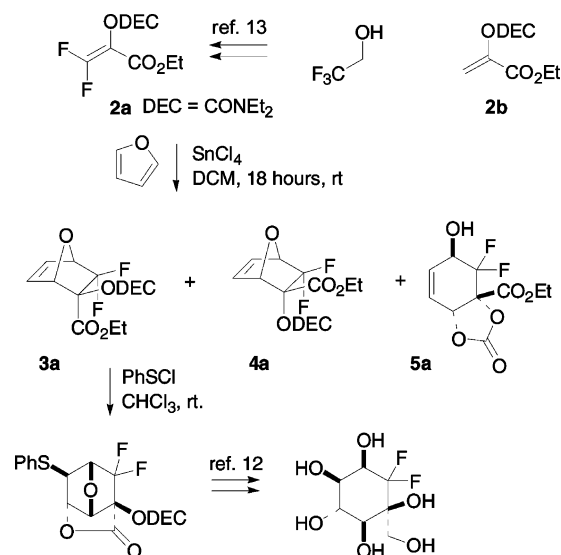
The uncatalyzed and catalyzed reactions delivered moderate (up to 40%) yields of cycloadducts, and **1a** was approximately an order of magnitude more reactive than ethyl acrylate **1b** in the uncatalyzed reaction, the reaction with the non-fluorinated dienophile taking over 1 month to reach 20% conversion of starting material. Unfortunately Wakselman was unable to ring open the cycloadducts without concomitant aromatization, and so the rich potential of these bicyclic species could not be realized.

Other researchers have synthesized simpler fluoroalkenes and explored their Diels–Alder chemistry both computationally and experimentally; these studies, which invariably involve cyclopentadiene (or even an isobenzofuran) as the 4 π electron component, have revealed that solitary fluorine atoms exhibit null or negative effects on the rates of cycloadditions.⁸ Whereas geminal CF₂ centers are known⁹ to exert strong positive effects on the rates of rearrangement reactions in which they rehybridize from sp² to sp³, less is known about the corresponding effects on cycloaddition reactions.

We prepared **2a** using metallated difluoroenol chemistry and found that tin(IV) chloride was the most effective catalyst for the cycloaddition with furan and substituted furans from a fairly diverse set of Lewis acids.¹⁰ The cycloadducts have been elaborated to analogues of (hydroxymethyl)conduritolols using sulfur electrophile chemistry and a reductive desulfonative ring opening reaction (Scheme 2).^{11,12}

The reactions with 2-methyl, 3-methyl, and 2,3-dimethylfuran were completely regioselective and rapid, reaching 100% conversion to cycloadducts after 45 min at 0 °C. With one exception (that of 3-methylfuran, which affords an 8:1 *endo*/*exo* mixture), stereoselectivities were rather low (ca. 3:1 *endo*/*exo* for furan, ca. 1:1 for 2-methyl- and 2,3-dimethylfuran).¹³

Scheme 2



We were intrigued by the high reactivity of the substituted furans; there seemed to be relatively few examples of their effective Diels–Alder reactions in the literature, and those examples involved the most reactive dienophiles such as maleic anhydride¹⁴ and DMAD.¹⁵ The report that 2,3-dimethylfuran affords a conjugate adduct with acrolein and other enals¹⁶ seemed particularly interesting, as did the very slow reactions between 2-methylfuran and α -chloroacrylonitrile under zinc(II)-catalyzed conditions.¹⁷ We synthesized **2b** and exposed it to furan and 2,3-dimethylfuran in the presence of the tin catalyst; **2b** was recovered unchanged after 7 days, indicating a significant reactivity difference between the CF₂ and CH₂ congeners. We were also anxious to explain the high level of regiochemical control in the reaction and the fate of the *exo*-cycloadduct **4a** from the reaction between furan and **2a** at a higher (stoichiometric) loading of tin(IV) chloride. *Endo*-cycloadduct **3a** and cyclic carbonate **5a** were the sole products under those conditions, raising a number of issues about how a tin(IV) species binds to a molecule with as many potential donor sites as **2a**.

Density functional theory (DFT) treatments have revealed some unexpected characteristics of well-known cycloaddition reactions, particularly in terms of the timing of formation of the two new C–C σ bonds formed in the reaction.¹⁸ For example, Domingo and co-workers have shown that cyclopentadiene reacts with a range of cyanoethenes *via* highly asynchronous transition states which have more in common with conjugate addition reactions than with the familiar picture of the classical concerted Diels–Alder cycloaddition.¹⁹ Earlier spectroscopic work by Sustmann and co-workers²⁰ appeared to identify zwitterionic intermediates in the stepwise reaction

- (7) (a) Leroy, J.; Molines, H.; Wakselman, C. *J. Org. Chem.* **1987**, *52*, 290. Ring opening raises a range of issues; for a recent example, see: (b) Chung, K. H.; Lee, H. G.; Choi, I. Y.; Choi, J. R. *J. Org. Chem.* **2001**, *66*, 5937.
- (8) (a) Ernet, T.; Maulitz, A. H.; Wurthwein, E. U.; Haufe, G. *J. Chem. Soc., Perkin Trans. 1* **2001**, 1929. (b) Essers, M.; Muck-Lichtenfeld, C.; Haufe, G. *J. Org. Chem.* **2002**, *67*, 4715.
- (9) (a) Wang, S. Y.; Borden, W. T. *J. Am. Chem. Soc.* **1989**, *111*, 7282. (b) Getty, S. J.; Borden, W. T. *J. Am. Chem. Soc.* **1991**, *113*, 4334.
- (10) (a) Crowley, P. J.; Moralee, A. C.; Percy, J. M.; Spencer, N. S. *Synlett* **2000**, 1737. (b) Non-fluorinated dienophiles related structurally to **9b** have been reported, but they react only with the more reactive dienes; see: Funk, R. L.; Yost, K. J. *J. Org. Chem.* **1996**, *61*, 2598. Ishihara, K.; Nakano, K. *J. Am. Chem. Soc.* **2005**, *127*, 10504.
- (11) Crowley, P. J.; Fawcett, J.; Kariuki, B. M.; Moralee, A. C.; Percy, J. M.; Salafia, V. *Org. Lett.* **2002**, *4*, 4125.
- (12) Crowley, P. J.; Fawcett, J.; Griffith, G. A.; Moralee, A. C.; Percy, J. M.; Salafia, V. *Org. Biomol. Chem.* **2005**, *3*, 3297.
- (13) Arany, A.; Crowley, P. J.; Fawcett, J.; Hursthouse, M. B.; Kariuki, B. M.; Light, M. E.; Moralee, A. C.; Percy, J. M.; Salafia, V. *Org. Biomol. Chem.* **2004**, *2*, 455.

- (14) Sneden, A. T. *Synlett* **1993**, 313.
- (15) Moss, G. P.; Keat, O. C.; Bondar, G. V. *Tetrahedron Lett.* **1996**, *37*, 2877.
- (16) Francke, W.; Reith, W. *Tetrahedron Lett.* **1981**, *22*, 2029.
- (17) (a) Kernen, P.; Vogel, P. *Helv. Chim. Acta* **1993**, *76*, 2338. (b) For structure–activity relationships in this reaction, see: Schuda, P. F.; Bennett, J. M. *Tetrahedron Lett.* **1982**, *23*, 5525. (c) For a recent example, see: Chen, J. C.; Zheng, G. J.; Zhang, C.; Fang, L. J.; Li, Y. L. *Chin. J. Chem.* **2003**, *21*, 904.
- (18) Domingo, L. R.; Picher, M. T.; Aurell, M. J. *J. Phys. Chem. A* **1999**, *103*, 11425.
- (19) Domingo, L. R.; Aurell, M. J.; Perez, P.; Contreras, R. *J. Org. Chem.* **2003**, *68*, 3884.
- (20) Sustmann, R.; Tappanchai, S.; Bandmann, H. *J. Am. Chem. Soc.* **1996**, *118*, 12555.

between π -donor activated butadienes and highly electron-deficient ethylenes.

In addition to the fundamental significance of the Diels–Alder cycloaddition and the long history of contention concerning the electronic mechanism of the reaction,²¹ there are very practical imperatives to understanding the timing of bond making events in processes of this type. The Diels–Alder reaction can be used to construct highly functionalized molecules containing multiple stereogenic centers concisely, so considerable effort has been expended toward the design of asymmetric processes in which chiral catalysts are used to deliver highly enantioselectively enriched materials.²² The design of processes of this type demands an accurate knowledge of the spatial properties of the transition state, the mutual proximities of various substrate groups, and the environments occupied by the Lewis acid catalysts.

We have previously used electronic structure methods to understand the origins of stereochemical control in the additions of crotyltin reagents to aldehydes rather successfully,²³ rationalizing the interplay between reagent structure and reaction stereoselectivity. The questions we set out to answer through this study concern the details of the interaction between **2a** and the tin(IV) catalyst, the timing of the σ -bond forming reactions, and, indeed, the concerted *versus* stepwise nature of the cycloaddition, the origins of the regioselectivity of the reactions, the factors underlying the significant reactivity difference between **2a** and **2b**, the effect of furan structure on reaction rate, and the mechanism of the conversion of *exo*-cycloadduct **4a** into **5a**.

Computational Methodology

Our approach is to employ mainly DFT and the hybrid B3LYP functional,²⁴ using the program GAUSSIAN (G98 and G03),²⁵ all structures being properly characterized as minima or transition structures. We have used two basis sets, the smaller (SDD),²⁶ being initially used to locate the stationary points of interest (reactants, products, and transition states) on the potential energy surface for the reaction of the unsubstituted furan with **6a**, in the absence of solvent. These structures were then used as starting points for the calculations with the larger basis set (6-31G**²⁷). For the Lewis acids other than SnCl₄ and AlCl₃, only the SDD basis set was employed. In all calculations we represented the dienophiles by **6a** or **6b**, which differ from the actual molecules studied experimentally only in the substitution of methyl for ethyl groups, in order to facilitate the computations; the smaller model **6c** was used for selected higher level *ab initio* calculations (Chart 1).

Chart 1

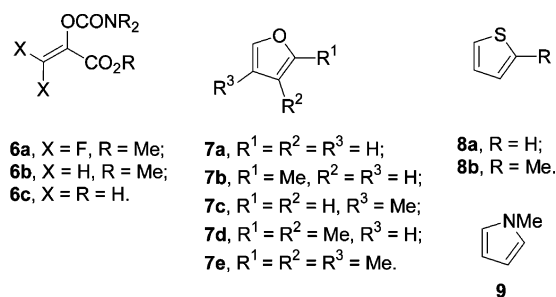


Table 1. Barrier and Reaction Energy (kJ mol⁻¹) for Model *exo*-Reaction between Furan and **6c**

method	ΔE_B	ΔE_R
BD(T)	104	-51
B3LYP	105	-4
MP2	73	-66
MP3	118	-52
MP4(DQ)	122	-55
HF	177	-27

We have studied the Diels–Alder reactions between dienophiles **6a** and **6b** and a series of furans **7a–e**, having varying degrees of methyl substitution, and the related heteroarenes **8a**, **8b**, and **9**. To determine the reactant and product structures we found that it was often necessary to start the geometry optimization from the transition state region. In the case of the reactant this leads to two loosely interacting molecules (the furan and the dienophile), whose potential energy surface is very flat, making a precise determination of the minima on these surfaces quite difficult, and necessitating the use of cutoff criteria which were less stringent than the default values for geometry optimization. Solvation effects were included using the polarizable continuum model (PCM) which provides an estimate of the free energy of solvation (solvent = dichloromethane, dielectric constant = 8.93, atomic radii are from the united atom topology model).²⁸ Subsequently, we studied the ring opening of some of the *exo*-cycloadducts employing the same approach as that for the Diels–Alder reactions (B3LYP/6-31G**).

To assess the performance of the B3LYP/6-31G** level of theory, we carried out a set of energy calculations on a small model system consisting of furan and the dienophile **6c**, in which the N- and O-methyl groups had been replaced by hydrogen atoms. This model was chosen to be of a sufficiently small size to allow study by quite high level *ab initio* methods which include explicit electron correlation (MP2, MP3, MP4(DQ), and BD(T)). The stationary structures of the model system were determined at the B3LYP/6-31G** level, and the energies of these structures were then evaluated using the series of *ab initio* methods and a 6-31G** basis.

Results and Discussion

Accuracy of the B3LYP Functional. Before considering the reaction of furan and the dienophiles, we evaluated the performance of the B3LYP/6-31G** method for modeling these reactions, by comparison with the results from correlated *ab initio* methods. The barrier heights (ΔE_B) and reaction energies (ΔE_R) for the *exo*-cycloaddition reaction, calculated by several theoretical methods, are presented in Table 1.

The Brueckner Doubles (BD(T)) result was taken as the benchmark of accuracy. The B3LYP barrier agrees closely with

- (21) (a) Dewar, M. J. S.; Olivella, S.; Stewart, J. J. P. *J. Am. Chem. Soc.* **1986**, *108*, 5771. For recent papers discussing aspects of the Diels–Alder mechanism, see: (b) Handoo, K. L.; Lu, Y.; Parker, V. D. *J. Am. Chem. Soc.* **2003**, *125*, 9381. (c) Ujaque, G.; Norton, J. E.; Houk, K. N. *J. Org. Chem.* **2002**, *67*, 7179.
- (22) Hayashi, Y. Catalytic Asymmetric Diels–Alder Reactions. In *Cycloaddition Reactions in Organic Synthesis*; Kobayashi, S., Jørgensen, K. A., Eds.; Wiley VCH: Weinheim, 2002; Chapter 1, pp 5–53.
- (23) Vincent, M. A.; Hillier, I. H.; Hall, R. J.; Thomas, E. J. *J. Org. Chem.* **1999**, *64*, 4680.
- (24) Becke, A. D. *J. Chem. Phys.* **1993**, *98*, 1372.
- (25) Frisch, M. J. et al. *Gaussian 2003*, version B.4; Gaussian, Inc.: Pittsburgh, PA, 2003.
- (26) (a) Dunning, T. H.; Hay, P. J. In *Modern Theoretical Chemistry*; Schaefer, H. F., Ed.; Plenum Press: New York, 1977. Vol. 3, pp 1–27. (b) Igel-Mann, G.; Stoll, H.; Preuss, H. *Mol. Phys.* **1988**, *65*, 1321.
- (27) (a) Ditchfield, R.; Hehre, W. J.; Pople, J. A. *J. Chem. Phys.* **1971**, *54*, 724. (b) Hehre, W. J.; Ditchfield, R.; Pople, J. A. *J. Chem. Phys.* **1972**, *56*, 2257. (c) Hariharan, P. C.; Pople, J. A. *Theor. Chim. Acta* **1973**, *28*, 213. (d) The Sn basis set was a modification of the one given in: Stromberg, A.; Gropen, O.; Walhgren, U. *J. Comput. Chem.* **1984**, *4*, 181. See the Supporting Information. (e) Francl, M. M.; Pietro, W. J.; Hehre, W. J.; Binkley, J. S.; Gordon, M. S.; Defrees, D. J.; Pople, J. A. *J. Chem. Phys.* **1982**, *77*, 3654.

- (28) Cances, M. T.; Mennucci, V.; Tomasi, J. *J. Chem. Phys.* **1997**, *107*, 3032. (b) Cossi, M.; Barone, V.; Cammi, R.; Tomasi, J. *Chem. Phys. Lett.* **1996**, *255*, 327. (c) Barone, V.; Cossi, M.; Tomasi, J. *J. Comput. Chem.* **1998**, *19*, 404. (d) Cossi, M.; Barone, V. *J. Chem. Phys.* **1998**, *109*, 6246. (e) Tomasi, J.; Persico, M. *Chem. Rev.* **1994**, *94*, 2027.

Table 2. Calculated (B3LYP/6-31G**) Activation (ΔG^\ddagger) and Reaction (ΔG°) Free Energies (kJ mol^{-1}) at 298 K for Dienophile/Furan Reactions, Giving *exo* (X) Or *endo* (N) Products^a

Entry	Diene	Dienophile	Catalyst	Solvent	$\Delta G^\circ_{\text{N}}$	$\Delta G^\ddagger_{\text{N}}$	$\Delta G^\circ_{\text{X}}$	$\Delta G^\ddagger_{\text{X}}$
1	7a	6a	No	No	19 (-16)	134 (106)	19 (-17)	133 (105)
2			No	Yes	5	111	12	117
3			Yes	No	18 (-12)	106 (82)	24 (-11)	113 (87)
4		6b	No	No	41 (9)	139 (115)	31 (5)	133 (110)
5			No	Yes	40	132	33	123
6			Yes	No	38 (7)	111 (85)	35 (0)	107 (79)
7	7b	6a	Yes	No	23 (-7)	80 (59)	22 (-8)	82 (65)
8	7c	6a	Yes	No	6 (-23)	88 (66)	3 (-26)	89 (71)
9	7d	6a	Yes	No	15 (-14)	71 (53)	17 (-15)	77 (53)
10	7e	6a	Yes	No	8 (-21)	63 (44)	9 (-22)	66 (47)
11	8a	6a	Yes	No	36 (2)	144 (116)	40 (6)	145 (117)
12	8b	6a	Yes	No	36 (5)	121 (95)	39 (8)	108 (85)
13	9	6a	Yes	No	78 (47)	87 (68)	77 (46)	79 (58)

^a The values in parentheses are the corresponding enthalpies for reactions without solvent.

this result, and only the HF and MP2 results diverge significantly, with the MP3 and MP4(DQ) barriers falling within $\pm 20 \text{ kJ mol}^{-1}$ of the BD(T) result. However, ΔE_{R} is poorly described at the B3LYP level, being exothermic by only 4 kJ mol^{-1} compared to the value 51 kJ mol^{-1} given at the BD(T) level. Thus, although ΔE_{B} is well described at the B3LYP level, this method appears to be better at describing the reactants rather than the products. In contrast, the MP2, MP3, and MP4(DQ) methods do considerably better at predicting the reaction energy.

Stationary Structures and the Role of SnCl_4 Catalyst.

Next, we considered the reactions of **6a** and **6b** with the unsubstituted furan, **7a**, first in the absence of the Lewis acid or solvent, so that their roles may be understood (Table 2). The effect of catalyst and variation of diene and dienophile are very similar whether free energies or enthalpies are considered, although the greater entropy of the reactants results in ΔG being greater than the corresponding ΔH value. Previous studies of

hetero-Diels–Alder reactions by Domingo and Andres²⁹ have highlighted the possibility of a two-step reaction rather than a concerted one and have identified the role of hydrogen bonding solvents such as chloroform in stabilizing zwitterionic intermediates.

In Table 3 we show the lengths of the two forming C–C bonds and some useful atomic and group charges for a number of transition states and intermediates, for example, see Figure 1.

For the uncatalyzed reaction between **6a** and **7a**, we found only a single transition state (confirmed by following the potential energy surface from the transition state to reactant and product). Table 2 (entry 1) with free energy barriers of 133 and 134 kJ mol^{-1} for the formation of the *exo* and *endo* products, respectively.

(29) (a) Polo, V.; Domingo, L. R.; Andres, J. *J. Phys. Chem. A* **2005**, *109*, 10438.
(b) Domingo, L. R.; Andres, J. *J. Org. Chem.* **2003**, *68*, 8662.

Table 3. Lengths (Å) of the Two Forming Bonds (C₅–C_B and C₂–C_A) and Charges (e) of the Fragments (Furan and SnCl₄) and of Atom (C_A), for *exo*-Reactions^a

entry	structure	catalyst	solvent	C ₅ –C _B	C ₂ –C _A	furan	C _A	SnCl ₄
1	6a-7a (TS)	no	no	1.90	2.50	+0.16	+0.09	–
2	6a-7a (TS)	no	yes	1.83	2.71	+0.28	+0.09	–
3	6a-7a (TS)	yes	no	1.79	2.74	+0.32	+0.08	–0.35
6	6b-7a (TS)	yes	no	1.80	2.65	+0.30	+0.22	–0.36
14	6a-7a (TS1)	yes	yes	1.99	3.17	+0.41	+0.10	–0.49
14	6a-7a (INT)	yes	yes	1.62	3.34	+0.68	+0.04	–0.54
14	6a-7a (TS2)	yes	yes	1.62	2.46	+0.49	+0.01	–0.49
7	6a-7b (TS)	yes	no	1.88	3.08	+0.37	+0.11	–0.36
16	6a-7b (TS1)	yes	yes	2.06	3.18	+0.39	+0.10	–0.48
16	6a-7b (INT)	yes	yes	1.59	3.43	+0.75	+0.03	–0.56
16	6a-7b (TS2)	yes	yes	1.60	2.33	+0.47	0.00	–0.48

^a C_A and C_B are the carbon atoms of the olefin double bond, with C_B being attached to the two hydrogen or fluorine atoms. Entries are labeled as those in Table 2 and 4.

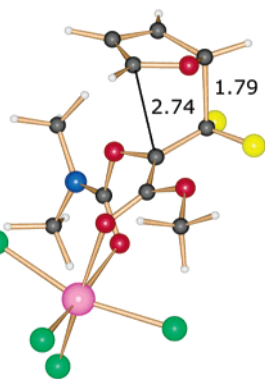


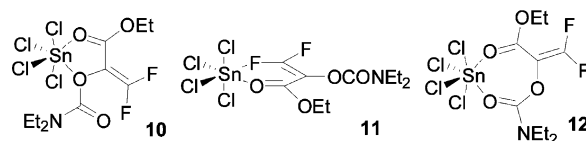
Figure 1. Transition state for the reaction of furan **7a** with fluorinated dienophile **6a** in the presence of SnCl₄ and in the absence of solvent.

The transition states for these reactions are very asynchronous in the C–C bond forming events, with one bond being close to fully formed (C–C lengths in the *exo* and *endo* transition states of 1.90 and 1.91 Å, respectively), only 122% of the final lengths (1.56 Å for both *exo* and *endo* product minima), while the other bond has barely begun to form (C–C lengths of 2.50 and 2.46 Å for the *exo* and *endo* forms, respectively).

The Mulliken charges indicate that 0.16 electrons have been transferred from furan to the dienophile (for both *exo* and *endo* transition states), showing the polar nature of the transition state. The carbon atom of the furan ring with the largest positive charge is one of those forming a C–C bond, but it is the longer of the two forming bonds. Entries 1 and 4 of Table 2 show that changing the CF₂ (**6a**) group for a CH₂ group (**6b**) in the dienophile exerts no significant change on the barrier height. However, it appears that the products derived from the CF₂ alkenoate **6a** are more stable than those from the corresponding CH₂ alkenoate **6b**, although the formation of both is still unfavorable with respect to the reactants. This difference in product stability is in line with the greater stability of fluorine bound to an sp³ rather than sp² carbon, so presumably the difference between these systems reflects the well-known destabilizing effect exerted upon sp² centres by a pair of fluorine atoms, which has often been invoked to explain the high reactivity of fluorinated systems in sigmatropic rearrangement reactions.³⁰ Given our model results (Table 1), this failure to predict an exergonic reaction is not unexpected. We have further calculated the MP2 energies at the MP2/6-31G**//B3LYP/6-

(30) Black, K. A.; Wilsey, S.; Houk, K. N. *J. Am. Chem. Soc.* **2003**, *125*, 6715.

Chart 2



31G** level, followed by their correction for thermodynamic and zero-point effects (using B3LYP/6-31G** values) and for the 15 kJ mol^{–1} overestimation of the reaction energy by MP2 (Table 1). The reaction free energies thus obtained for the CF₂ congener are –20 and –19 kJ mol^{–1} for the *exo* and *endo* products, respectively, while the corresponding values for the CH₂ species are –7 and 0 kJ mol^{–1}. These results show clearly that the reaction is exergonic for the CF₂ dienophile but is essentially ergonically neutral for the CH₂ form.

Understanding the catalyzed reaction requires that we know the nature of the interaction between the Lewis acid and the dienophile. Dienophile **2a** could act as a bidentate ligand in a number of different ways; there are opportunities for the formation of the five-, six-, and seven-membered-ring chelate structures **10**, **11**, and **12**, respectively. Metal–fluorine interactions have been invoked in a number of reaction systems,³¹ so **11** (a type of complex which cannot be generated from **2b**) must be considered, given the strikingly different reactivities of the two dienophiles (Chart 2).

There is little in the literature to predict how the Lewis acid would bind to **2a** and **2b**. A search of the Cambridge Structural Database³² revealed only five- and six-membered³³ chelates involving stannic chloride. Denmark³⁴ has obtained structures for *bis*-phosphoramidate ligand–stannic chloride complexes though these include much larger rings. Our calculations (using **6a**) predict a chelate of type **12** to be the lowest energy minimum structure; structures corresponding to **10** and **11** are not minima, with the carbonyl-bound five-coordinate tin complexes being lower in energy. In **12** the catalyst pins the plane of the alkoxy-carbonyl group close to that of the difluoroalkene (the angle between the two π-planes is 16.7°). The size of the tin(IV) makes it an ideal metal to include in the seven-membered chelate of type **12**, but other factors are also important. The calculated binding free energies give equilibrium constants for the reaction of SnCl₄ with our modified dienophiles **6a** and **6b** (in dichloromethane) of 0.14 and 0.56, respectively. The first value is consistent with experiment, where relatively high loadings of catalyst (ca. 15% or above) of SnCl₄ have to be used before the reaction proceeds at a reasonable rate.³⁵ The combined inductive effects of the two fluorine atoms presumably make complex formation with the Lewis acid less favorable than that for **6b**.

- (31) (a) Mohanta, P. K.; Davis, T. A.; Gooch, J. R.; Flowers, R. A. *J. Am. Chem. Soc.* **2005**, *127*, 11896. (b) Nakamura, Y.; Okada, M.; Sato, A.; Horikawa, H.; Koura, M.; Saito, A.; Taguchi, T. *Tetrahedron* **2005**, *61*, 5741. (c) Itoh, Y.; Mikami, K. *Org. Lett.* **2005**, *7*, 649. (d) Itoh, Y.; Yamanaka, M.; Mikami, K. *J. Am. Chem. Soc.* **2004**, *126*, 13174. (e) Ding, H.; Friestad, G. K. *Org. Lett.* **2004**, *6*, 637. (f) Ooi, T.; Kagoshima, N.; Uraguchi, D.; Maruoka, K. *Tetrahedron Lett.* **1998**, *39*, 7105. (g) Ooi, T.; Kagoshima, N.; Maruoka, K. *J. Am. Chem. Soc.* **1997**, *119*, 5754. (h) Hanamoto, T.; Fuchikami, T. *J. Org. Chem.* **1990**, *55*, 4969.
- (32) Fletcher, D. A.; McMeeking, R. F.; Parkin, D. *J. Chem. Inf. Comput. Sci.* **1996**, *36*, 746.
- (33) For an example of related six-ring chelation, see: Denmark, S. E.; Bui, T. *Proc. Natl. Acad. Sci. U.S.A.* **2004**, *101*, 5439.
- (34) Denmark, S. E.; Fu, J. P. *J. Am. Chem. Soc.* **2003**, *125*, 2208.
- (35) The preliminary screen was described in ref 10a; further results are described in the Supporting Information.

We have investigated the possibility that other Lewis acids could bind in a similar way to SnCl_4 and catalyze the transformation. We have studied the reaction between the fluorine containing dienophile **6a** and furan **7a** in the presence of catalyst, but without solvent, using the smaller (SDD) basis. We find that the Lewis acid ZrCl_4 does indeed catalyze the reaction, reducing the free energy barrier from 129 to 89 kJ mol^{-1} (B3LYP/SDD). However, while computational studies predict zirconium(IV) chloride to be an effective catalyst consistent with the similar ionic radii of zirconium(IV) and tin(IV), our experimental studies for the actual reaction in neat furan were disappointing. The catalyst even failed to promote the cycloaddition reaction between **2a** and 2,3-dimethylfuran in dichloromethane, instead returning a conjugate adduct of chloride with **2a**. Clearly chloride displacement from this metal is considerably easier than the loss of chloride from the tin(IV) species.

A different mode of coordination was predicted between **6a** and aluminum trichloride, with the formation of a monodentate complex, binding of AlCl_3 being exclusively to one carbonyl group. However, experimentally, our initial *endo* selective cycloadditions (*endo/exo* 8:1) used diethylaluminum chloride, but the conditions were unacceptable for synthesis (neat furan, 30 °C, 14 days for complete conversion).

Table 2 also presents the results for SnCl_4 -catalyzed formation of cycloadducts from the CH_2 and CF_2 alkenoates. The free energy barrier is lowered for all reactions irrespective of whether or not the dienophile is fluorinated, or whether *exo* or *endo* products are formed. The CF_2 alkenoate favors *endo* products (barrier heights of 113 and 106 kJ mol^{-1} for *exo* and *endo* products, respectively, entry 3), consistent with experiment in spite of the lack of solvent in the model used, while the CH_2 alkenoate favors *exo* products (barrier heights are 107 and 111 kJ mol^{-1} for *exo* and *endo* products, respectively, entry 6). As for the corresponding uncatalyzed reaction, only a single transition state was found for reaction of the unsubstituted furan in the presence of the catalyst (Figure 1).

However, there are important changes in both the structure and the charge distribution in the transition state for the catalyzed reaction compared to the uncatalyzed reaction (Table 3). The charge on the furan ring is increased significantly in the transition states compared to the uncatalyzed reaction, ranging from 0.30 to 0.34 in the former, compared to 0.13–0.16 in the latter. For the uncatalyzed reaction, the developing C–C bonds are in the ranges 1.90–1.96 Å and 2.35–2.50 Å, while for the catalyzed reaction the corresponding values are 1.76–1.80 Å (ca. 115% of the final bond length of 1.56 Å for both the *exo* and *endo* transition states) and 2.58–2.74 Å. Clearly the Diels–Alder reaction is highly asynchronous without a catalyst, but much more so in the presence of the Lewis acid. An overlay of the calculated transition states for **6a** and **6b** (furan, SnCl_4) reveals only minor differences in geometry between the CH_2 and CF_2 cases (Figure 2).

In the transition state of the reaction of **6a**, the charge lost from the furan ring should formally reside on the carbon atom (C_A) of the double bond without the fluorine atoms. However, the adjacent carbonyl group is well-aligned to stabilize the developing charge on both dienophiles (**6a** and **6b**) effectively, and the bonding to the positively charged tin accentuates the electron-withdrawing effect of the carbonyl group, giving carbon atom C_A a positive charge. The two C–F bonds have little effect

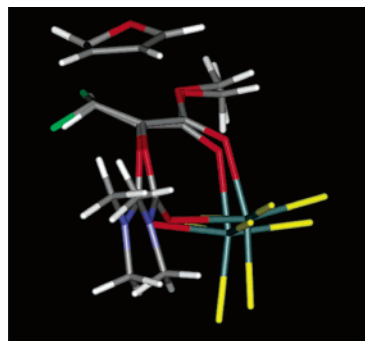


Figure 2. Overlay of calculated transition states leading to *exo*-cycloadducts for **6a** and **6b** in the presence of SnCl_4 and absence of solvent.

on the structure and charge distribution of the transition state, but only an inductive effect would actually be expected, which may not produce a significantly different transition state geometry.

There is the possibility of biradicaloid contributions to the transition state of Diels–Alder reactions. Both dienophiles examined in this study are formally captodative,³⁶ bearing both π -donor and π -acceptor groups on the same alkenyl carbon. This combination of substituent groups is often associated with a propensity to undergo biradical reactions. Difluoroalkenes are also known to undergo formal [2+2]-cycloaddition reactions *via* biradical pathways at relatively low reaction temperatures (cyclobutane products indicate the intervention of these pathways strongly).³⁷ Vogel and Kernen rationalized the regiochemical outcome of 2-methylfuran cycloaddition on the basis of biradical character,^{17a} but we found no evidence whatsoever for the intervention of such a pathway despite allowing the possibility explicitly in the DFT calculations. It is possible that the known bias of the DFT method to favor charge separated species³⁸ may mask the true nature of these reactions, but we believe that the large effect exerted by the powerful Lewis acid tin(IV) points toward a strongly polarized transition state rather than one involving unpaired electrons. The small model system **6c** was examined by looking at the magnitude of the contribution of the second-most important electron configuration in the BD-(T) wavefunction; its value (0.1) was sufficiently small to indicate there is only a very small amount of biradical character.

Role of Solvent. The effect of solvent on the uncatalyzed and catalyzed reaction was modeled employing the PCM method²⁸ with the dielectric constant for dichloromethane. The free energy barrier was lowered whether the Lewis acid is present or not (Tables 2 and 4), in line with the considerable zwitterionic nature of the transition states. Again, only a single transition state is found for the unsubstituted furan in the presence of solvent, but in the absence of catalyst. However, if the Lewis acid is present, the barrier lowering is significantly

- (36) (a) For a review, see: Viehe, H. G.; Janousek, Z.; Merenyi, R.; Stella, L. *Acc. Chem. Res.* **1985**, *18*, 148. For recent examples, see: (b) Antonietti, F.; Gambarotti, C.; Mele, A.; Minisci, F.; Paganelli, R.; Punta, C.; Recupero, F. *Eur. J. Org. Chem.* **2005**, 4434. (c) Bagal, S. K.; Adlington, R. M.; Brown, R. A. B.; Baldwin, J. E. *Tetrahedron Lett.* **2005**, *46*, 4633. (d) Smith, Q.; Huang, J. Y.; Matyjaszewski, K.; Loo, Y. L. *Macromolecules* **2005**, *38*, 5581. (e) Maiti, A.; Gerken, J. B.; Masjedizadeh, M. R.; Mimieux, Y. S.; Little, R. D. *J. Org. Chem.* **2004**, *69*, 8574. (f) Adam, W.; Schulte, C. M. *Eur. J. Org. Chem.* **2004**, 1482. (g) Cruz, M. D.; Tamariz, J. *Tetrahedron Lett.* **2004**, *45*, 2377.
- (37) Cyclobutane formation by fluoroalkene dimerization under relatively mild conditions has been described in: (a) Kobayashi, S.; Yamamoto, Y.; Amii, H.; Uneyama, K. *Chem. Lett.* **2000**, 1366. (b) Yamamoto, M.; Swenson, D. C.; Burton, D. J. *Macromol. Symp.* **1994**, *82*, 125.
- (38) Smith, A.; Vincent, M. A.; Hillier, I. H. *J. Phys. Chem. A* **1999**, *103*, 1132.

Table 4. Calculated (B3LYP/6-31G**) Free Energies (kJ mol⁻¹) at 298 K, Relative to Reactants, of the First (TS1) and Second (TS2) Transition States and of the Intermediate (INT), for the Reaction of **6a**, with Furans (**7a**, **7b**, **7c**, **7d**), in the Presence of Catalyst and Solvent

entry	diene	product	$\Delta G^{\ddagger}_{TS1}$	ΔG°_{INT}	$\Delta G^{\ddagger}_{TS2}$
14	7a	<i>exo</i>	69	55	75
15	7a	<i>endo</i>	64	46	71
16	7b	<i>exo</i>	54	24	58
17	7b	<i>endo</i>	52	23	58
18	7c	<i>exo</i>	47	27	49
19	7c	<i>endo</i>	52	27	56
20	7d	<i>exo</i>	49	17	49
21	7d	<i>endo</i>	46	13	48

greater (Tables 2 and 4), and now two transition states are found for the unsubstituted furan (Tables 3 and 4, Figure 3).

The structure of the corresponding zwitterionic intermediate is quite distinct from that of the two transition states, having one nearly fully formed bond and essentially no incipient formation of the second bond. The reaction is now a clearly defined two-step process, with the first transition state (TS1) leading to the formation of the first C–C bond in the intermediate (INT) and the second transition state leading to the second C–C bond. It is interesting to see that the intermediate has more zwitterionic character than either of the two transition states (Table 3). If we take the first transition state, we find that the solvent lowers the free energy barrier by 16 kJ mol⁻¹ for the reaction in the absence of the Lewis acid which leads to *exo* products with the CF₂ alkenoate **6a** (Table 1, entries 1, 2) and by 44 kJ mol⁻¹ with the Lewis acid present (Tables 2, 4; entries 3, 14). This is due to the increased zwitterionic character of the transition state of the catalyzed reaction, which is further stabilized by the polar solvent. For example, the large dipole moment of the *exo* transition state (17.1 D) is increased to 24.3 D in the presence of solvent. This effect is also evident from a Mulliken analysis (Table 3), which reveals an increase in electron density on SnCl₄ with the chlorine atoms gaining 0.2e, and a corresponding loss of density from the furan ring of 0.09e (*exo* transition state). Clearly the Lewis acid creates a large dipole moment that is favored in the more polar solvents. Calculations were also carried out using the PCM model for solvents whose dielectric constants bracket that of dichloromethane ($\epsilon = 8.93$); these were THF ($\epsilon = 7.58$) and 1,2-dichloroethane ($\epsilon = 10.36$); a linear relationship between ΔG^{\ddagger} and dielectric constant (ϵ) was observed, consistent with the highly polarized nature of the model transition state.

Reactivity of Methylated Furans and Related Heteroarenes. Methylation of the furan diene would be expected to lead to stabilization of the charge separated transition state since methyl groups have the effect of stabilizing carbenium ions and free radicals strongly. We therefore examined the effect of various methyl substitution patterns on the SnCl₄ catalyzed Diels–Alder reaction. Table 2 (entries 7–10) summarizes the results for mono- (2- or 3-) **7b** and **7c**, di- (2,3-) **7d**, and tri- (2,3,4-) **7e** methyl furans; the results confirm the expected effect, with the respective free energy barriers for *exo* and *endo* transition state formation decreasing from 113 and 106 kJ mol⁻¹ for unsubstituted furan, to 66 and 63 kJ mol⁻¹ for the trimethylated analogue. In these reactions the carbon of the furan that is closest to the alkenoate in the transition state is never methylated. A much smaller reduction in barrier is found if the

substituted furans are reacted in this alternative regiochemical sense; for example, the barrier is 94 kJ mol⁻¹ instead of the 77 kJ mol⁻¹ calculated for the experimentally observed orientation of 2,3-dimethyl furan (Scheme 3). One of the methyl groups is attached directly to the electrophilic carbon (the carbon next to oxygen of furan that has the longest bond to the alkenoate) in the observed regiochemical pathway, whereas when a methyl group is not attached to that centre, as in the alternate pathway, a higher barrier is observed (Scheme 3). This effect of stabilization by 2-methyl substitution (at the electrophilic carbon) rather than 3-methyl substitution is also seen in the lower barrier calculated for **7b** compared to that for **7c**. A similar stabilizing effect of methyl substitution at the 2-position of furan has been previously observed.³⁹

The effect of solvent on the tin(IV)-catalyzed reaction of **7b** follows our findings for the reaction of furan itself (Table 3). The free energy barrier is lowered considerably by the presence of solvent, although the actual lowering is some 10–20 kJ mol⁻¹ less for the methyl substituted furan. In the presence of solvent the reaction is predicted to be stepwise rather than concerted (Table 4) with the second transition state either similar in energy or only a few kJ mol⁻¹ higher than the first.

However, B3LYP may have a tendency to artificially favor charge separated species.³⁸ To verify that our zwitterionic intermediates are not a result of this, we have verified for one of these species that it does not collapse to reactant or product under geometry optimization by an *ab initio* method which includes electron correlation. However, the size of our intermediates, with the Lewis acid present, prevented us from employing the BD(T) method used to assess B3LYP for our model system, which does not have such an intermediate on its potential energy surface. We have employed the Complete Active Space (CAS) SCF method⁴⁰ to study the intermediate arising from reactants **7e** and **6a** with the Lewis acid SnCl₄ being present. This active space had eight electrons in eight orbitals which included both the vacant orbital on the “furan fragment” involved in formation of the C₂–C_A bond and the orbital (partly located on C_A) donating electrons to form this bond. Geometry optimization of the zwitterionic intermediate with this wavefunction which gave 1764 configurations (employing the 6-31G** basis set) confirmed this structure to be stable.

The results of the calculations of the reaction of the fluorinated dienophile (**6a**) with *N*-methylpyrrole (**9**), thiophene (**8a**), and 2-methylthiophene (**8b**) in the presence of the SnCl₄ catalyst, but without solvent, are given in Table 2 (entries 11–13). The barriers for the two thiophenes are similar to those for furan and methyl furan. However, both reactions are considerably more endergonic than that of furan. Although we have not carried out higher level calculations similar to those we have reported for furan, if B3LYP similarly underestimates the stability of the products, both reactions are still likely to be unfavorable. We note that the predicted endergonicity is even larger for *N*-methylpyrrole.

Structure Reactivity Relationships. The calculations described so far have provided insight into the potential energy

- (39) Domingo, L. R.; Aurell, M. J. *J. Org. Chem.* **2002**, *67*, 959. The regiochemistry of the cycloaddition between a masked *ortho*-benzoquinone and 2-methylfuran was studied previously by DFT. Our results are consistent with the reported outcomes.
- (40) (a) Frisch, M.; Ragazos, I. N.; Robb, M. A.; Schelgel, H. B. *Chem. Phys. Lett.* **1992**, *189*, 524. (b) Klene, M.; Robb, M. A.; Frisch, M. J.; Celani, P. *J. Chem. Phys.* **2000**, *113*, 5653.

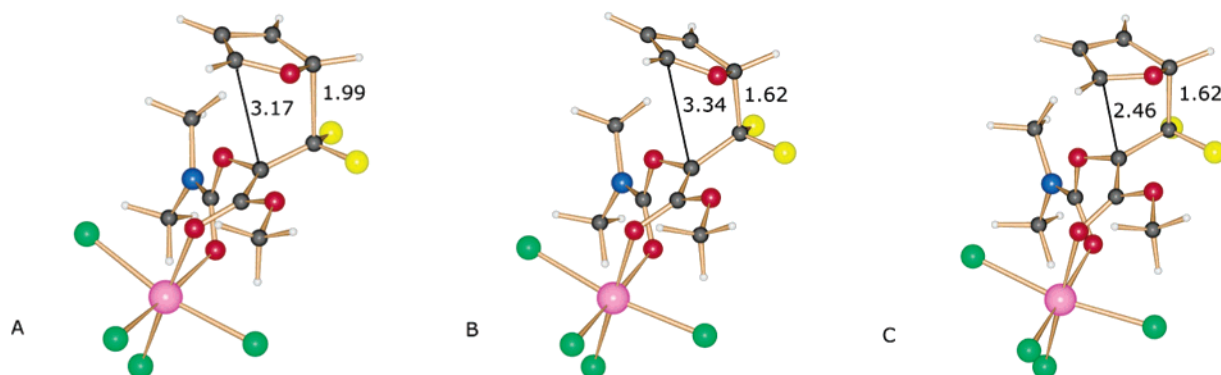
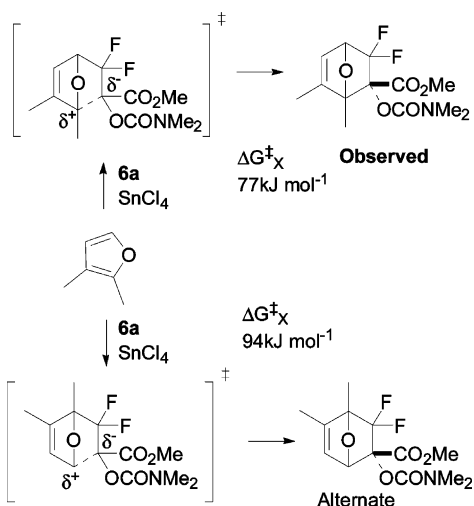


Figure 3. Transition states and intermediate for reaction of furan **7a** with fluorinated dienophile **6a**, in the presence of both SnCl₄ catalyst and solvent (entry 14): (A) transition state 1 (TS1); (B) intermediate (INT); (C) transition state 2 (TS2).

Scheme 3. Different Regiochemical Pathways Available for the Reaction of **6a** with **7d**



surface involved in these Diels–Alder reactions and how the surface is modified by catalyst, solvent, and variation of the diene. In particular the presence of solvent predicts a clear change in mechanism. The strong zwitterionic nature of the first transition state is common to both concerted and stepwise pathways, but the zwitterionic intermediate appears to occupy a deeper well as methyl groups are added. We now explore the extent to which the quantitative differences in reactivity can be predicted and whether this can lead to empirical structure–reactivity relationships which can be more widely used.

Measurement of relative cycloaddition rate constants was undertaken to obtain kinetic data which can be directly compared to our calculations, by following the disappearance of alkenoate for three of the furans by ¹⁹F NMR spectroscopy. We were unable to follow product appearance because the cycloadducts have broad ¹⁹F NMR spectra for all furans apart from **7a** making accurate integration of spectra impractical. Equimolar quantities of **2a** and the appropriate furan were mixed in a CD₂Cl₂ solution of stannic chloride (25 mol %) in the NMR tube. The reactions were followed in the probe of the spectrometer at 300 K; the total reaction time for the experiment was based on the synthetic results, and the entire reaction window filled with data points. Good decay kinetics were obtained; the data were fitted assuming second-order kinetics (first-order in **2a** and the furan with equal starting concentrations; see Supporting Information), yielding the total rate constants for disappearance of **2a** shown in Table 5.

For furan **7a**, the overall conversion of dienophile (ca. 70%) corresponded reasonably well to the yield of isolated purified products (54% total). The ratio of rate constants for product formation (*endo*-**3a**/*exo*-**4a**/carbonate **5a** = 17.4:6:1) corresponds well to the ratio of isolated yields (*endo*-**3a**/*exo*-**4a**/carbonate **5a** = 19:7:1) indicating that the NMR conditions represent the synthetic conditions quite accurately. The failure of the reaction to consume the dienophile completely is attributed to exhaustion of the furan diene through polymerization; the rapid formation of strongly colored material and its presence in the crude reaction mixture is consistent with this. The isolated synthetic yields and total consumption of dienophile also correspond well for the more substituted furans.

We have included rate data for 3-methylfuran **7c** but have excluded it from the correlations because of its exceptional *endo* stereoselectivity (8:1).¹² However, our calculations for 3-methylfuran (**7c**) predict a definite preference for the *exo* product (Table 4) in contrast to our experimental data. In the experimental reaction of **2a**, the transition state for the *exo*-pathway involves a degree of steric crowding between the methyl group on the furan and one of the *N*-ethyl groups in the carbamate; this can only be relieved by rotating the plane of the sp² carbamoyl group nitrogen and losing the stabilization which arises from amide resonance. However, this crowding is reduced in our calculations where the ethyl group of **2a** has been replaced by a methyl group in **6a**, thus artificially favoring formation of the *exo*-product.

Correlations between rate constants and calculated reaction barriers require the extraction of the separate rate constants for the diastereoisomeric cycloaddition pathways. The rate constants *k*_{endo} and *k*_{exo} were estimated assuming *k*₂ (the total rate constant for disappearance of alkenoate) is given by

$$k_2 = k_{exo} + k_{endo}$$

and

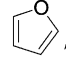
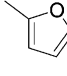
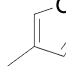
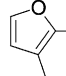
$$k_{exo}/k_{endo} = \% \text{ } exo/\% \text{ } endo$$

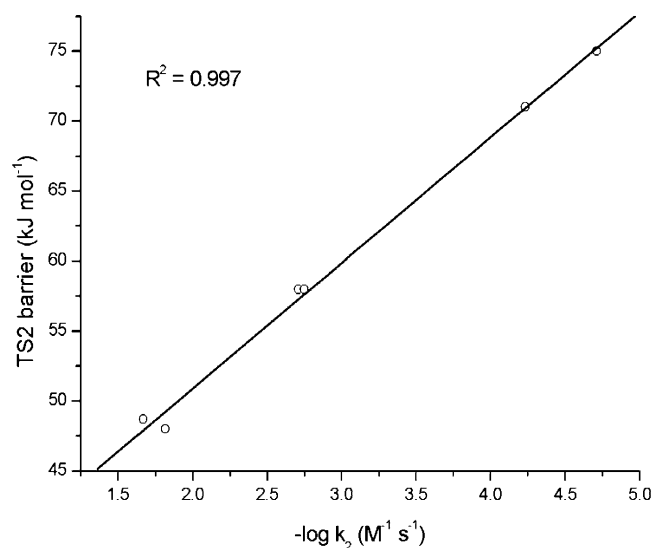
so

$$k_{endo} = k_2/(1 + (\% \text{ } exo/\% \text{ } endo))$$

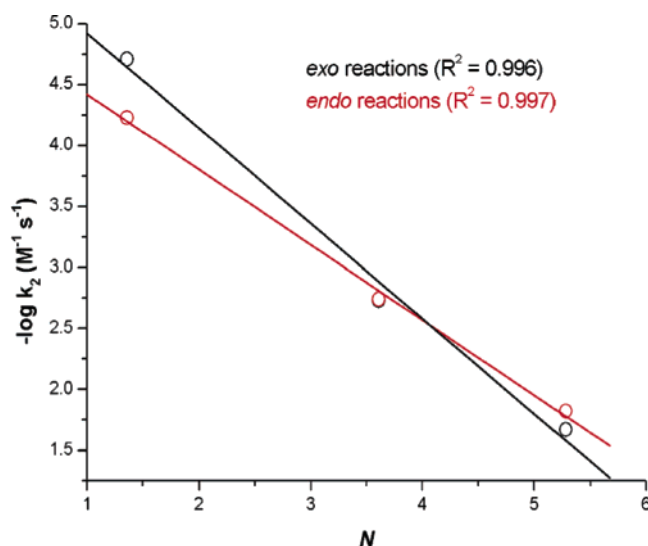
and similarly to obtain *k*_{exo}. This treatment yields the additional data in Table 5.⁴² The overall good correlation between theory and experiment is illustrated in Figure 4 where the logarithm of the rate constant is plotted against the free energy barrier,

Table 5. Rate Data for the Cycloadditions with Furans **7a**, **7b**, **7c**, and **7d** in CD₂Cl₂ at 300 K

Furan	 7a	 7b	 7c	 7d
Parameter				
$10^5 k_2$ (M ⁻¹ s ⁻¹)	7.81	372	695	3677
$10^5 k_{exo}$ (M ⁻¹ s ⁻¹)	1.952	186	77	2148
$-\log k_{exo}$ (M ⁻¹ s ⁻¹)	4.71	2.73	3.11	1.67
$10^5 k_{endo}$ (M ⁻¹ s ⁻¹)	5.86	186	618	1529
$-\log k_{endo}$ (M ⁻¹ s ⁻¹)	4.23	2.73 (6)	2.21	1.82
<i>N</i>	1.36	3.61	(-)	5.28 ^a

^a Reference 41.**Figure 4.** Correlation between calculated free energy barriers and cycloaddition rates for separated *endo*- and *exo*-cycloadduct forming reactions.

TS2. As the energies of the two transition states which we have identified in the presence of both catalyst and solvent are only separated by ~ 4 kJ mol⁻¹, we cannot definitively assign the first or second bond-forming step as rate determining, so we have chosen somewhat arbitrarily to use TS2 in Figure 4. Thus the free energy barriers predict the important features of our kinetic data. The introduction of the first methyl group (**7b**, **7c**) produces a considerable lowering of the barrier, the second methyl group (**7d**) producing a smaller effect. The prediction of the stereochemical preference is a rather more stringent test of the theory. The free energy barriers (Table 4) do indeed predict the observed preference for the *endo* product in the case of the reaction of furan itself, with a calculated difference in the barrier heights of less than 5 kJ mol⁻¹. This difference is predicted to be generally smaller for the methyl-substituted furans, **7b** and **7d**, also in line with our measurements.

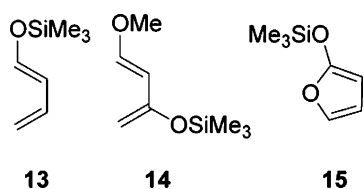
**Figure 5.** Linear correlation of the measured second-order rate constant for the reaction of **2a** with furans, with Mayr's *N* parameter.

We turn now to more qualitative structure–reactivity relationships. The classical picture of the structure/reactivity relationship in Diels–Alder reactions compares diene_{HOMO} and dienophile_{LUMO} energies⁴³ within a concerted reaction; given the strongly polar character of these reactions, it would seem more appropriate to consider the relationship among the π -nucleophilicity parameters (*N*) obtained by Mayr and co-workers,^{41,44} reaction rates, and calculated energy barriers. Parameters are available for furan **7a** (1.36), 2-methylfuran **7b** (3.61), and 2,3-dimethylfuran **7d** (5.28).⁴¹ These values derive from LFER's for the reactions between various diarylcarbenium and π -nucleophiles ranging from simple alkenes to silyl ketene acetals. Good (though limited to three points) correlations were obtained between $-\log k_{exo}$, $-\log k_{endo}$, and *N* (Figure 5) suggesting strongly that the reaction rate is indeed controlled

(41) Westermaier, M.; Mayr, H. Unpublished results, personal communication to J.M.P.

(42) This quantity can be measured directly for the reaction with furan **7a** (the total *exo* rate is given by the rate of formation of **4a** and **5a**, as **5a** is made from **4a**, *vide infra*). Our earlier synthetic work¹³ looked for evidence of reversibility in the Diels–Alder reaction and found none, so we believe that the treatment of the reactions as essentially irreversible under kinetic control is justified.(43) (a) Fleming, I. *Frontier Orbitals and Organic Chemical Reactions*; J Wiley and Sons: Chichester, 1976; p 113. (b) Sustmann, R.; Schubert, R. *Angew. Chem., Int. Ed.* **1972**, *11*, 840.(44) (a) Gotta, M. F.; Mayr, H. *J. Org. Chem.* **1998**, *63*, 9769. (b) Burfeindt, J.; Patz, M.; Muller, M.; Mayr, H. *J. Am. Chem. Soc.* **1998**, *120*, 3629. (c) Herrlich, M.; Mayr, H.; Faust, R. *Org. Lett.* **2001**, *3*, 1633. For reviews of this work, see: (d) Mayr, H.; Ofial, A. R. *Pure Appl. Chem.* **2005**, *77*, 1807. (e) Mayr, H.; Kempf, B.; Ofial, A. R. *Acc. Chem. Res.* **2003**, *36*, 66. (f) For the computational construction of an alkene electrophilicity scale, see: Domingo, L. R.; Perez, P.; Contreras, R. *Tetrahedron* **2004**, *60*, 6585.

Chart 3



by the ease with which the furans can sustain the development of positive charge and consistent with the decidedly zwitterionic mechanism.

Our synthetic studies of the Diels–Alder reaction have shown that while furans react with alkenoate **2a** under mild tin(IV)-catalyzed conditions, other highly electron-rich dienes undergo conjugate addition reactions leading to release of fluoride ion and the formation of complex mixtures of products from which we have failed to characterize discrete compounds. These dienes include 1-(trimethylsilyloxy)-1E,3-butadiene **13**, Danishefsky's diene **14**, and 1-(trimethylsilyloxy)furan **15** (Chart 3). We also failed to form cycloadducts from the reaction between **2a** and **8a**, **8b**, or **9** under our normal conditions (25 mol % SnCl₄, DCM, rt). Starting material was recovered from the reaction with the thiophenes, while conjugate addition prevailed in the case of the pyrrole.

Understanding the relationship between diene structure and reactivity and the outcome of cycloaddition reactions is a key goal if we are to be able to develop new synthetic strategies based on **2a** and related species, and a simple relationship between *N* and reaction outcome would be extremely useful; however, there is no such simple relationship when a wider class of dienes is examined. Parameters are also available for 1-(trimethylsilyloxy)-1E,3-butadiene **13** (4.60), 1-(trimethylsilyloxy)furan **15** (7.22), Danishefsky's diene **15** (8.57),⁴⁴ and 2,3-dimethylfuran **7d** (5.28).⁴¹ The comparison between the reactions of the various furans suggests that there may be a maximum nucleophilicity, even for cyclic dienes above which conjugate addition occurs instead of cycloaddition.

This scenario is represented in the Jencks–More O'Ferrall diagram⁴⁵ of Figure 6; alkyl substitution on the furan stabilizes the bottom right-hand corner of the diagram strongly resulting in an anti-Hammond or perpendicular effect on the transition state for the concerted asynchronous reaction. When this stabilization becomes sufficient (the zwitterionic intermediate **16** exists in a definite potential well), the reaction pathway becomes stepwise, leaving the inner square of the diagram and crossing into the wings. At this point, failure to capture the zwitterion internally because of an unfavorable conformation, or because of excessive cation stabilization, sets the stage for fluoride ion loss and side product formation. Strong zwitterion solvation also may result in strong lowering of the bottom right-hand corner. The correlations suggest strongly that the three furan substrates react by the same highly asynchronous mechanism, *via* a transition state which lies either very close to the lower right-hand corner of the Jencks–More O'Ferrall diagram or more likely in the wings and *via* **16**. The reactions are unproductive at lower π -nucleophilicity for acyclic dienes because they are not locked in the conformations required for

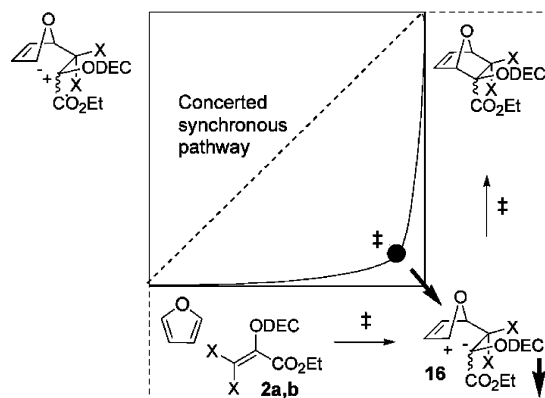


Figure 6. Jencks–More O'Ferrall diagram showing concerted and stepwise pathways and anticipating movement of the transition state and the shift to a two-step mechanism in response to carbenium ion stabilization (solid arrows).

cycloaddition, so that whereas the cycloaddition is rapid and high yielding for 2,3-dimethylfuran (*N* = 5.28), the less π -nucleophilic and extremely synthetically useful 1-(trimethylsilyloxy)-1E,3-butadiene (*N* = 4.60) fails to produce any significant quantity of cycloadduct. The behavior of *N*-methylpyrrole (*N* = 5.85) is of interest given that it has the *s-cis* diene arrangement required for cycloaddition; however pyrroles usually require electron-withdrawing *N*-protecting groups to prevent ligation or attack by the lone pair, so the synthetic failure of this diene is predated. The transition to a conjugate addition reaction which diverts away from cycloaddition appears to have been reached at 1-(trimethylsilyloxy)furan (*N* = 7.22) (Figure 7).

The failure of the thiophenes to react is more surprising if the reaction is thought of as a highly polar addition rather than a cycloaddition. Thiophenes are extremely unreactive dienes in the Diels–Alder reaction because the loss of aromaticity opposes the reaction strongly.⁴⁶ However, thiophenes are more competent nucleophiles in Friedel–Crafts reactions; 2-methyl thiophene and furan have very similar π -nucleophilicities demonstrated by their *N* values, but the thiophene failed to return any cycloadduct under our conditions, even when a full equivalent of tin(IV) was added. Again, ligation of the Lewis acid may well explain this observation.

Overall, the Mayr *N* measures the ability of the furan to progress to the zwitterion by reacting as a nucleophile with the alkenoate. The *endo* and *exo* rate constants correlate well with the calculated energies for the second barrier (TS2), consistent with the existence of the zwitterion as an intermediate on the energy surface, and its closure becoming rate determining. This model is consistent with our explanation for the failure of a number of synthetically useful and reactive but acyclic dienes to form cycloadducts; they progress to the zwitterion, but the need for conformational change makes other nonproductive pathways more favorable. The agreement between the calculated reaction barriers and the kinetic outcomes is remarkable, given the difficulty of calculating meaningful energy barriers for a range of reactions using DFT.^{47,48}

(45) For recent applications of this powerful tool, see: (a) Lee, K.; Sung, D. D. *Curr. Org. Chem.* **2004**, *8*, 557. (b) Buncel, E.; Albright, K. G.; Onyido, I. *Org. Biomol. Chem.* **2004**, *2*, 601. (c) Schramm, V. L. *Acc. Chem. Res.* **2003**, *36*, 588.

(46) (a) Kotsuki, H.; Nishizawa, H.; Kitagawa, S.; Ochi, M.; Yamasaki, N.; Matsuoka, K.; Tokoroyama, T. *Bull. Chem. Soc. Jpn* **1979**, *52*, 544. (b) Kotsuki, H.; Kitagawa, S.; Nishizawa, H.; Tokoroyama, T. *J. Org. Chem.* **1978**, *43*, 1471. (c) Iddon, B. *Heterocycles* **1983**, *20*, 1127. (d) For recent developments, see: Kumamoto, K.; Fukada, I.; Kotsuki, H. *Angew. Chem., Int. Ed.* **2004**, *43*, 2015.

(47) Lynch, B. J.; Truhlar, D. G. *J. Phys. Chem. A* **2001**, *105*, 2936.

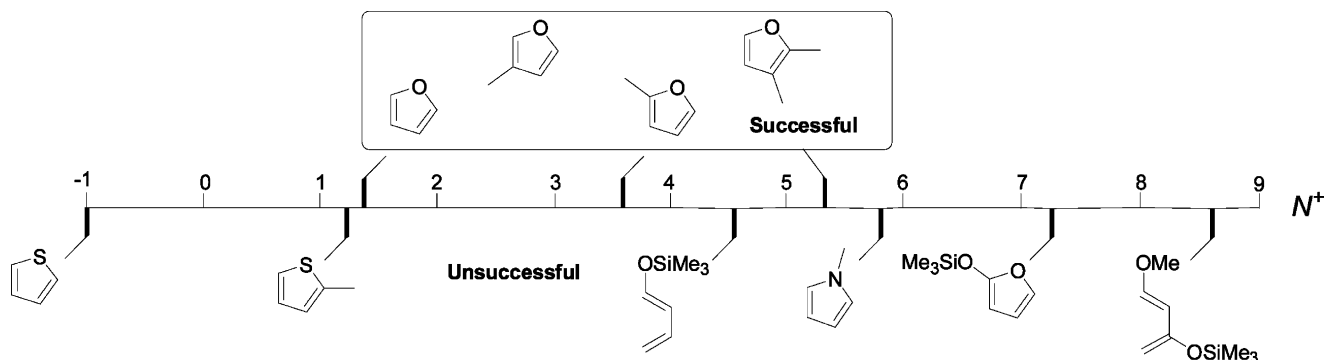
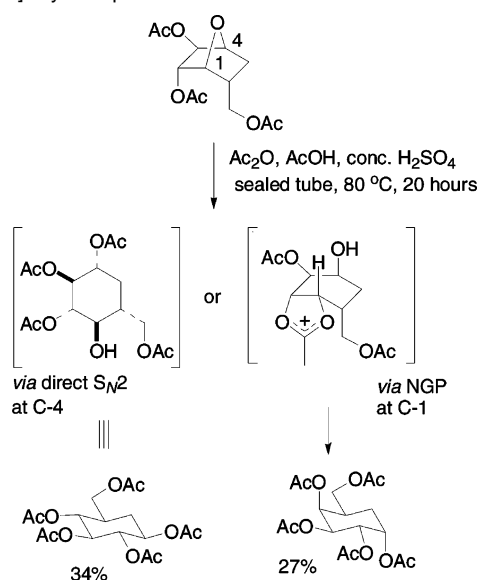


Figure 7. Selected acyclic and cyclic dienes, their N values, and the relationship to the cycloaddition outcome.

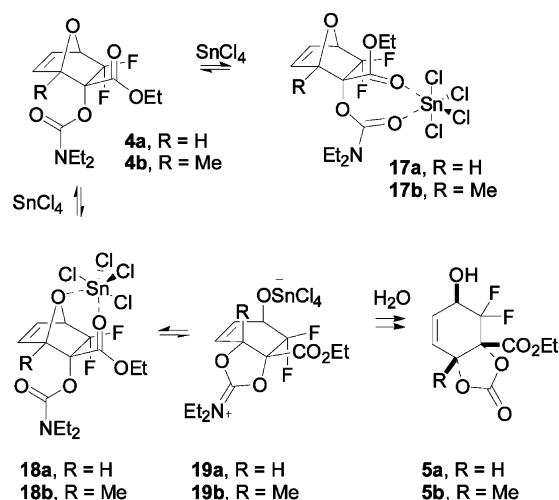
Scheme 4 Neighboring Group Participation by an Ester Carbonyl Group during the Solvolytic Ring Opening of an Oxa[2.2.1]bicycloheptane



Possibility of Cyclic Carbonate Formation. Another intriguing aspect of this chemistry concerned a slow and low yielding side reaction under the catalytic tin(IV) conditions; we detected the formation of cyclic carbonate **5a** in the reaction between **2a** and **7a**. Formally, this product could arise from the intramolecular nucleophilic attack by the carbonyl oxygen of the *exo*-cycloadduct **4a**, on the adjacent bridgehead carbon. This type of neighboring group participation by acetoxy groups is known and has been used by Ogawa *inter alia* in syntheses of a number of carbasugar molecules.⁴⁹ The conditions for these reactions are often rather forcing; Scheme 4 shows an example.

Though **4a** is considerably less electron-rich than molecules in the literature which undergo this type of cleavage, the scissile bond is allylic, suggesting that the appropriate coordination of a Lewis acid to the bridging ether oxygen could start to polarize the C–O bond and enlist the carbamate oxygen as a nucleophile. However, the bridging ether oxygen is the least basic Lewis site of the three potential donor oxygens. We were able to grow crystals of **17a** and solve the crystal structure.⁵⁰ Clearly this cannot be an intermediate on a direct pathway to **5a**.

Scheme 5. Curtin–Hammett Mechanism for the Formation of Cyclic Carbonate **5a**



To trigger ring opening, stannic chloride must first bind to the bridging ether oxygen, which is a poor donor. To compensate for this, six-membered chelate formation (in **18a**) involving carbonyl and ether oxygen donors, which is impossible from the *endo*-cycloadduct, is proposed. Bridge cleavage, which is strain relieving, may then occur reversibly.

The proposed intermediate **19a** progresses to **5a** when hydrolysis removes it from the equilibrium (Scheme 5). Non-aqueous workup of a reaction solution followed by ¹⁹F NMR revealed the exclusive presence of **4a**: we were only able to observe **5a** after aqueous workup. Substituted 2-methyl- and 2,3-dimethylfurans behaved quite differently, failing to return cyclic carbonates. Instead, only *exo*-cycloadducts were obtained, and all attempts to force the reactions led to decomposition.

We have used DFT (B3LYP/6-31G**) calculations to follow the mechanism of the transformation of **20a** and **20b** to **22a** and **22b**, via the intermediates **21a** and **21b**, respectively (Chart 4).

The free energies of the solvated (DCM) complexes **20a** and **21a** differed by 19 kJ mol⁻¹ in favor of **20a**, confirming that the proposed equilibrium between these species and therefore the Curtin–Hammett mechanism was viable. The proposed intermediate **22a** was confirmed as an energy minimum, and the transition structure linking it to reactant **21a** was located, the barrier being 74 kJ mol⁻¹. This transition structure showed a high degree of bond cleavage (C–O = 2.06 Å), suggesting

(48) Vincent, M. A.; Palmer, I. J.; Hillier, I. H.; Akhmatkaya, E. *J. Am. Chem. Soc.* **1998**, *120*, 3431.

(49) (a) Ogawa, S.; Yoshikawa, M.; Taki, T.; Yokoi, S.; Chida, N. *Carbohydr. Res.* **1995**, *269*, 53. (b) Ogawa, S.; Iwasawa, Y.; Nose, T.; Suami, T.; Ohba, S.; Ito, M.; Saito, Y. *J. Chem. Soc., Perkin Trans. 1* **1985**, 903. (c) Baran, A.; Kazaz, C.; Secen, H.; Sutbeyaz, Y. *Tetrahedron* **2003**, *59*, 3643.

(50) Fawcett, J.; Moralee, A. C.; Percy, J. M.; Salafia, V.; Vincent, M. A.; Hillier, I. H. *Chem. Commun.* **2004**, 1062.

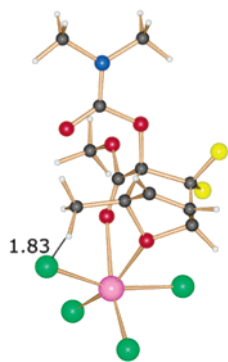
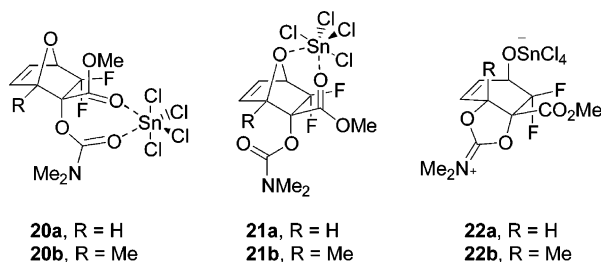


Figure 8. Calculated structure of **21a** modified by the presence of the C-2 methyl group.

Chart 4



that the unfavorable effect of methylation at the bridgehead position is steric rather than electronic; it was anticipated that the presence of the methyl group at C-2 would assist the C–O cleavage by stabilizing the incipient carbenium ion. The calculations were repeated for the methylated molecules to investigate this further. Complex **20b** was more stable than **21b** by 58 kJ mol⁻¹, with the barrier to the formation of **22b** (from **18b**) being 63 kJ mol⁻¹. Thus, the total barrier to the transition state, with reference to the more stable **20b**, is 121 kJ mol⁻¹, which compares to a barrier for the unsubstituted case of 93 kJ mol⁻¹. Figure 8 shows the calculated structure of **21a** modified by the presence of the C-2 methyl group. One of the chlorine ligands is very close to the methyl group (2.27 Å from the methyl centroid); it is this interaction which is responsible for the significant change in the balance of energies between the two scenarios. Unfortunately, this limits the potential of what appeared to be an extremely concise and very useful rapid method for progressing *exo*-cycloadducts to very highly functionalized and differentially protected cyclohexene polyols.

Conclusions

We have used electronic structure calculations to understand important aspects of the Diels–Alder reaction between the dienophiles **6a** and **6b** (and therefore the experimental reactions of **2a**) and a number of furans. First, we find that the forward barriers for both dienophiles are very similar. The difference in

outcome between the reactions of the fluorinated and non-fluorinated dienophiles arises because the barrier to the back reaction (cycloreversion) is higher in the fluorinated case. This is primarily an enthalpic effect of fluorine atoms on alkene stability so the cycloaddition outcome may be said to be subject to thermodynamic control. The additional stability for products arising from **6a** compared to **6b** is due to the removal of the energetically unfavorable difluoroalkene moiety in the Diels–Alder product of **6a**. With respect to the products, we have noted the inadequacy of the B3LYP functional to properly predict the exothermicity of the reaction for the fluorine containing dienophile **6a**. This is yet a further example of the B3LYP approach underestimating the energies of reactions which involve C–C bond formation.⁵¹ However, the rates of reaction of the different furans are kinetically controlled by alkene substituent effects on a zwitterionic intermediate and the two transition states that lie close to it. The zwitterionic nature of the transition state is evident in all our studies. Both the Lewis acid and methyl substitution increase the zwitterionic nature of the transition state, leading to enhanced interaction with the polar solvent, thereby increasing the rate. When both solvent and catalyst are present, such stabilization leads to a definite two-step rather than a highly asynchronous concerted reaction, with the two transition structures being very close in energy. Although the gas-phase barrier is essentially the same for both *endo*- and *exo*-reactions, the inclusion of catalyst allows the calculation of reaction free energy barriers which correlate with experimental rate constants very well.

Different modes of Lewis acid binding to the cycloadduct were investigated, allowing the formation of a cyclic carbonate product to be rationalized. We were able to explain why only one of our cycloadducts underwent this reaction, by revealing an unanticipated highly unfavorable interaction between the C-2 alkyl group and one of the ligands at tin.

Acknowledgment. We thank the EPSRC (GR/M94922, fellowship for ACM) and the University of Leicester (studentship for RR). We also wish to acknowledge the use of the EPSRC's (Engineering and Physical Sciences Research Council) Chemical Database Service at Daresbury, Professor H. Mayr (Ludwig-Maximilians-Universitaet, Muenchen) for the *N* value for 2,3-dimethylfuran, and C. Hall (University of Leicester) for studying the effects of catalyst loading.

Supporting Information Available: Kinetic data, coordinates (angstrom) of stationary structures on the potential energy surface of the reaction of furan **7a** with dienophile **6a**. This material is available free of charge via the Internet at <http://pubs.acs.org>.

JA061458P

(51) Check, C. E.; Gilbert, T. M. *J. Org. Chem.* **2005**, *70*, 9828.